Published in final edited form as:
Virology. 2007 March 30; 360(1): 120–128.

Deletions within the 5′UTR of coxsackievirus B3: consequences for virus translation and replication

Isabelle P. Hunziker, **Christopher T. Cornell**, and **J. Lindsay Whitton***

Abstract

Key features of an ideal RNA-based vaccine against coxsackievirus B3 (CVB3) are (i) limited genome replication/virus production (to minimize vaccine-related pathology) and (ii) abundant virus protein synthesis (to maximize immunogenicity). These attributes may apply to CVB3 RNAs lacking up to 250 nucleotides (nt) from their 5′ terminus; these RNAs do not give rise to infectious progeny, but they have been reported to retain the entire CVB3 IRES (mapped to nt ~432-639) and to produce large quantities of viral protein in transfected cells. Here, we constructed five 5′ RNA deletion variants that, to our surprise, failed to protect against CVB3 challenge. We investigated the reasons for this failure, and conclude that: (i) a 5′ terminal deletion as short as 32 nt abolishes CVB3 RNA replication in transfected cells; (ii) this deleted RNA, and others with longer deletions, do not direct abundant protein synthesis in transfected cells, probably as a consequence of their replicative incapacity; and (iii) the CVB3 IRES is substantially larger than previously thought, and its 5′ boundary lies between residues 76 and 125, very closely approximating that of the poliovirus IRES.

Introduction

Coxsackievirus B3 (CVB3), a member of the genus Enterovirus within the family Picornaviridae, is an established human pathogen that causes heart disease (Woodruff, 1980; Reyes and Lerner, 1985; Kishimoto and Hiraoka, 1994), pancreatitis (Arnesjo *et al.*, 1976; Imrie *et al.*, 1977; Ramsingh, 1997; Mena *et al.*, 2000) and meningoencephalitis (Modlin and Rotbart, 1997; Daley *et al.*, 1998). These infections are difficult to treat and, to date, no approved vaccine is available. However, efforts have been made to develop a vaccine against CVB3. These include an inactivated vaccine (See and Tilles, 1994), several live attenuated viruses (Gauntt *et al.*, 1983; Fohlman *et al.*, 1993; Dan and Chantler, 2005), and DNA vaccines (Henke *et al.*, 1998). We have recently described an RNA vaccine, based on a mutated full-length viral genome, that conferred some degree of protection against disease (Hunziker *et al.*, 2004). In attempting to improve the efficacy of the RNA vaccine approach, we wished to generate a full-length genomic variant that would retain the capacity to direct the synthesis of abundant viral protein (thereby maintaining immunogenicity) but that would be unable to replicate (thus enhancing its safety). To design such a vaccine, we needed to know the boundaries of the various genomic elements that controlled replication and translation.

The CVB3 capsid is non-enveloped, and contains a single-stranded positive-sense RNA genome of ~7400 nucleotides (nt) in length (Genbank U57056: ref Knowlton *et al.*, 1996). The RNA molecule comprises a 5′ untranslated region (5′UTR) of 742 nt, followed by a single open reading frame of 6555 nt that encodes the ~220 kDa viral polyprotein, which is co- or post-

*Corresponding author: Molecular and Integrative Neurosciences Department, SP30-2110, The Scripps Research Institute, 10550 N. Torrey Pines Rd., La Jolla, CA 92037, USA, Tel: 858-784-7090, FAX: 858-784-7380, Email: lwhitton@scripps.edu.

translationally cleaved by virus-encoded proteases to generate the mature protein products. Translational initiation in eukaryotic cells usually requires that a pre-initiation complex attaches to the m7GpppN cap at the 5′ end of an mRNA, and moves along the molecule, in a process termed scanning, until it encounters the first potential translational initiation codon. Picornaviruses represent an exception to the general rules concerning ribosomal attachment. The mRNAs of these viruses are uncapped, and seminal studies revealed a structure within the 5′UTR that directed ribosomal entry and was named the internal ribosomal entry site (IRES, Jang *et al.*, 1988; Pelletier and Sonenberg, 1988; Pelletier *et al.*, 1988a). Most picornaviral IRES elements belong to one of two groups, which differ in sequence, secondary structure, and the location of the translational initiation codon. Enteroviruses (e.g., polioviruses and coxsackieviruses) and rhinoviruses contain a type I IRES, and the initiation codon is usually ~50-150 nucleotides (nt) downstream from the 3′ end of the ribosome binding site. The boundaries of the IRES, and the importance of specific sequences within the element, have been mapped for poliovirus; the results indicate that the motif encompasses nt ~140-631 (Meerovitch *et al*., 1991; Nicholson *et al.*, 1991). However, analyses of the CVB3 5′UTR have suggested (i) that the core IRES of this virus was located between nt 432-639, and thus was ~200 nt shorter than that of poliovirus and (ii) that, perhaps as a result of this apparently foreshortened IRES, the first 250 nt of the CVB3 5′UTR could be deleted with only a modest (~50%) reduction in viral protein synthesis in RNA-transfected cells (although virus production was abrogated) (Liu *et al.*, 1999). The phenotype of abundant protein synthesis in the absence of infectious virus production appeared ideal for a putative RNA vaccine, and led us to prepare, from the full-length CVB3 genome, five variant RNAs containing deletions in the 5′UTR. However, none of these variants conferred protection against disease in mice. This observation caused us to re-evaluate the sequences in the CVB3 5′UTR that regulate viral replication and protein synthesis.

Materials & Methods

Mice and tissue culture cells

Male C57BL/6 mice (H-2b MHC haplotype) were obtained from The Scripps Research Institute (TSRI) breeding facility. All animal experiments were approved by TSRI Animal Care and Use Committee. HeLa cells were used for virus titrations and RNA transfections, and were maintained in Dulbecco's modified Eagle medium (DMEM; GIBCO BRL, Invitrogen, Carlsbad, CA) supplemented with 10% fetal bovine serum (FBS), 2 mM L-glutamine, 100 U/ml penicillin, and 100 μg/ml streptomycin (complete DMEM).

Plasmids

The coxsackievirus B3 strain used is a plaque-purified isolate (designated H3, van Houten *et al.*, 1991) of the cardiopathogenic Woodruff strain of CVB3. The plasmid pH3, encoding a full-length infectious clone of this virus (Knowlton *et al*., 1996), was generously provided by Dr. Kirk U. Knowlton (University of California, San Diego), and was used as the parental plasmid for the construction of the various 5′UTR deletion variants pH3IH2-IH6.

In vitro transcription

The DNA templates (pH3, pH3IH2-IH6) were linearized with the restriction enzyme Cla I (New England Bio Labs, Beverly, MA), phenol-chloroform extracted, ethanol precipitated, washed with 70% ethanol and resuspended in sterile distilled water. One microgram of each DNA was used as a template for transcription based on the MEGAscript kit (uncapped RNA; Ambion, Austin, TX) according to the manufacturer's directions, then the template DNA was removed by the addition of 1 μl of DNase, followed by incubation at 37 °C for 15 min. RNA was recovered by ethanol precipitation.

In vivo RNA inoculation

RNA was suspended in sterile PBS at a concentration of 300 μg/ml, and 50 μl (15 μg) were injected into the tibialis anterior muscle of mice. For the studies of RNA infectivity, samples were harvested at the indicated times post-injection.

Organ preparation for titration and histology

The hearts, spleens, and pancreata were removed from the mice immediately after euthanasia. Each organ was divided into two approximately equal portions, one of which was placed into a cryotube and fast-frozen in dry ice for later virus titration. The other portion of each organ was fixed in 10% normal buffered formalin and processed for histological analyses. Five micron paraffin sections were prepared and stained with Masson's trichrome.

Plaque assays

HeLa cells were plated in six well plates (5–7.5 x 10^5 cells/well) and incubated at 37°C with 5% CO_2 for ~24 hours, at which time they reached ~70-90% confluency. The weight of each frozen organ sample was determined, then the tissue was homogenized in 1 ml of DMEM, and 10-fold serial dilutions were prepared in DMEM. Media was aspirated from the 6 well plates, and 400 μl of each serial dilution was added to individual wells. Plates were incubated at 37° C, with gentle rocking every 15 minutes. After 1 hour, cells were overlaid with 4 ml of 1x DMEM in 0.6% agar (1:1 mixture of 2x DMEM at 37°C and 1.2% agar at 55°C). At ~42 hours post-infection, cells were fixed in methanol:acetic acid (3:1 v/v), and agarose plugs were removed. The monolayers were stained with 0.5% crystal violet in 20% ethanol, rinsed in tap water, and plaques were counted. The titer (pfu/g of organ) was calculated based on the weight of each tissue sample.

Transfection of HeLa cells

To determine the infectious status of the RNA molecules and to evaluate viral protein production in tissue culture, HeLa cells (at about 70-80% confluency in a 6 well plate) were transfected with 3 μg of the indicated uncapped RNA using Lipofectin and OPTI-MEM (both GIBCO BRL, Invitrogen) according to the manufacturer's directions; in our hands, 25-50% of HeLa cells express the desired gene products after transfection of nucleic acids. After 3 h, the transfection mixture was aspirated and replaced by complete media; this time point defined the beginning of the post-transfection period.

Evaluation of virus protein synthesis in transfected cells

HeLa cells were transfected with uncapped RNA molecules as described above and, 16 hours later, were washed with saline and starved for 30 minutes in methionine- and cysteine-free DMEM containing 10% FCS at 37°C. 200 μl of ^{35}S-labeled amino acids (MP Biomedicals, Irvine, CA) were added (0.3 mCi/ml final activity), and a one-hour incubation at 37°C followed. Cells were resuspended in 30 μl of 1x SDS buffer, frozen, then boiled for 5 minutes, and applied to a 12.5% polyacrylamide gel, as described in the text. The gel was dehydrated with 3 washes using DMSO for 45 minutes each, and finally impregnated with 20% PPO in DMSO for 1 hour. Another wash in running H_2O followed for 1 hour, before the gel was dried on a gel-dryer at 65ºC overnight and finally exposed to a photographic film.

Evaluation of RNA replication by slot-blot

HeLa cells were transfected with RNA as described above and were harvested at 0, 3, 6, 12, and 24 h post-transfection. RNA was extracted using TRIzol LS Reagent (Invitrogen) according to the manufacturer's directions. All samples were dissolved in an aqueous solution containing 50% formamide (J.T. Baker Inc., Phillipsburg, NJ), 7% formaldehyde (Fisher

Scientific, New Jersey, NJ), and 1x SSC and incubated at 68 °C for 15 min. Then, two volumes of 20x SSC (Ambion) were added, and each RNA sample was loaded onto a nitrocellulose sheet in the slot-blot manifold. After washing twice with 10x SSC, the nitrocellulose was removed, air-dried, baked in a vacuum oven at 80 °C for 2 h, and finally crosslinked in a Stratalinker at 200 joules for 1 min. The nitrocellulose was pre-hybridized at 68 °C for 2h in 50% formamide, 6x SSC, 5x Denhardt's reagent, 0.5% SDS (Ambion), and 100 μg/ml boiled, denatured salmon sperm DNA. Radiolabeled probes, specific for either the genome or antigenome and produced based on the MAXIscript kit (Ambion), were added at 1 x 10^7 cpm/ml, and the blots were incubated at 68 °C for approximately 16 h, after which the nitrocellulose was washed three times: at RT using 1x SSC, 0.1% SDS; at 68 °C in 0.2x SSC, 0.1% SDS; and finally in 0.1x SSC, 0.1% SDS. The blot was exposed to a Kodak film at -70 °C with an intensifying screen for ~ 1-2 h. The intensities of the bands on the resulting autoradiograph were quantified using the public domain software ImageJ (available at the NIH web site http://rsb.info.nih.gov/ij/).

In vitro translation

In vitro translation reactions were carried out as described (Cornell *et al.*, 2004). Uncapped RNA was produced using the MEGAscript kit (Ambion). DNase treated transcripts were quenched with the addition of 375 μl of sodium dodecyl sulfate (SDS) stop buffer (0.5% SDS, 100 mM NaCl, 10 mM Tris-HCl [pH 7.5], 1 mM EDTA) and 100 μg of predigested proteinase K. The resulting mixture was incubated at 37 °C for an additional 30 min, phenol-chloroform extracted, and ethanol precipitated. RNA pellets were washed with 70% ethanol, dried, and resuspended in diethyl pyrocarbonate-treated water. All transcripts were quantified on an ethidium bromide-stained agarose gel by using RNA of the same length and known quantity as a standard. For the translation, 65% of S10 extract from suspension HeLa cells, 1x "All four" buffer [10x buffer: 10 mM ATP, 2.5 mM GTP, 2.5 mM UTP, 2.5 mM CTP, 600 mM potassium acetate, 300 mM creatine phosphate, 4 mg of creatine kinase per ml, 155 mM HEPES-KOH (pH 7.4)], 400 ng RNA, and 2 μl of ^{35}S-methionine (Amersham Biosciences, Piscataway, NJ) were mixed and used in 20 μl reactions. The HeLa S10 extract was generously provided by Prof. Bert L. Semler, University of California, Irvine. The translation was performed at 30 °C for 4 h, after which 2x lysis buffer was added, and the reactions were heated to 90 °C for 5 min. Ten μl of the reactions were loaded and run on a 12.5% polyacrylamide gel. The gel was dehydrated with three washes using DMSO for 45 min each, and finally impregnated with 20% PPO in DMSO for 1 h. Another wash in running H_2O followed for 1 h, before the gel was dried on a gel-dryer at 65 °C overnight and finally exposed to a photographic film.

Results

Generation of a family of 5′ deletion variants, based on a full-length infectious CVB3 genome

Based on published findings, CVB3 mutants bearing deletions outside the IRES (for example, deletion of residues 1-63, or of 1-249) should have minimal effect on translation in transfected cells, while viral infectivity should be completely abolished (Liu *et al.*, 1999). Because these qualities were well-suited to an RNA vaccine, we generated a series of deletions, varying in size between 32 nt and 209 nt, in the 5′UTR of an infectious full-length CVB3 genome. An infectious clone of the cardiopathogenic Woodruff strain of CVB3, pH3, was used as a parental plasmid for the construction of the deletion mutants by site-specific PCR-based mutagenesis. The 5′UTRs of pH3 and the resulting five variants, termed IH2-IH6, are shown diagrammatically in Figure 1A. The five regions targeted for deletion are color-coded, and the proposed "core" of the CVB3 IRES (nt 432-639) is shown as a grey box; all five deletions terminate >200 nt upstream of this area. RNA folding algorithms have been applied to the 5′ UTR of enteroviruses, and have revealed extensive secondary structure, some of which has

been experimentally confirmed. For the CVB3 5′UTR, it has been suggested that there may be 11 stem-loops (termed A-K), two of which (A & B) were predicted within the first ~100 bases; and deletion analyses indicated that sequences up to and including much of stem-loop E (which ends at residue 481) precede the 5′ boundary of the IRES (Liu *et al.*, 1999). For this reason, we applied the RNA folding predictive algorithm (the GeneQuest component of Lasergene software, DNAStar, Madison WI) to this region of the CVB3 5′UTR (Figure 1B), and the predicted structure – which differs from the above, but is similar to that of other enteroviruses such as poliovirus – is shown, with the stem-loops labeled I-IV. The locations of the 5 deletions relative to the proposed RNA folds are shown; none of them impinge on the complex structure previously termed stem-loop E, only the latter part of which lies within the proposed core of the CVB3 IRES.

All five variants fail to produce infectious virus, but none induces protective immunity

To maximize RNA vaccine safety, it is important that the production of infectious virus be minimized. Each of the six RNA molecules shown in Figure 1A was transfected into susceptible HeLa cells and, 48 hours later, the cells and supernatants were assayed for the presence of infectious virus; this was detected only following transfection of the wild-type (pH3) RNA (Figure 2A). To better evaluate the attenuation of these RNA molecules *in vivo*, 15 μg of each RNA was injected into the tibialis anterior muscle of mice (4 mice per RNA). Five days later, virus titers in heart, spleen and pancreas were measured. Virus was detected only in the tissues of mice that had received pH3 RNA. The titers in heart are shown in Figure 2B, and are representative of titers in all three organs. Furthermore, the direct *in vivo* injection of picornavirus RNA can result in pathology, if the RNA was derived from a pathogenic virus. As shown in Figure 2C, (left panel), dramatic pancreatitis was present 5 days after injection of pH3 RNA, but no pathology was observed following injection of any of the five variant RNAs (IH2 shown as example, right panel). All of these results were consistent with published data, and were generally desirable for candidate vaccines. Next, we evaluated the protective efficacy of the RNAs. 15 μg of each of the five variant RNAs were inoculated into C57BL/6 mice (4 per group). As a negative control, four mice were inoculated with 15 μg of an RNA encoding β-galactosidase. pH3 RNA was not used in this vaccination experiment, as it encodes wild-type virus, and causes disease (Figure 2C); therefore, as a positive control vaccine, an attenuated recombinant virus encoding enhanced green fluorescent protein was used; we have previously shown that this virus is non-pathogenic *in vivo*, but induces strong protective immunity (Hunziker *et al.*, 2004). Three weeks later, all mice received booster vaccinations identical to the originals, and three weeks thereafter, all mice were challenged with 8000 pfu of wild-type CVB3. Fecal titers were measured two days later (Figure 2D). Virus was undetectable in the mice that had been immunized with the attenuated rCVB-eGFP. In contrast, very high viral titers (10^8-10^9 pfu/gram) were present in recipients of each of the five candidate RNA vaccines, and were indistinguishable from those observed in recipients of β-galactosidase RNA. This failure of protection was unexpected, because CVB3 deletion variants lacking nt 1-63, or 1-249, have been reported to produce substantial quantities of viral protein (~50% of wild-type) following RNA transfection (Liu *et al.*, 1999). Consequently, we set out to identify the reason(s) for vaccine failure.

All five deletions in the 5′UTR dramatically reduce viral protein production in transfected cells

The most obvious reason for the lack of immunogenicity was that insufficient viral protein was synthesized by cells that had taken up the deleted RNAs. To address this possibility, the five variant RNAs, or pH3 RNA, were transfected into HeLa cells, and viral and host protein production was evaluated. Data for cells transfected with the IH2 and IH3 constructs are shown in Figure 3A; the results for the IH4-6 constructs were very similar. Virus proteins were readily detected in cells that had been transfected with pH3 RNA (viral proteins highlighted by dots),

but were undetectable in cells transfected with any of the RNA deletion mutants. Host cell proteins were present, and quite abundant, in all extracts from RNA-transfected cell populations; this is consistent with the fact that only a minority of cells in each preparation will have been successfully transfected. This result, although different from published data, is consistent with the observed vaccine failure. The absence of detectable viral proteins could be explained in several ways, including: (i) a difference in template abundance in transfected cells; (ii) reduced efficiency of translational initiation (if, for example, a deletion interfered with IRES function); or (c) a combination of the above.

Following transfection, the abundance of wt RNA increases, while that of the variant RNAs rapidly declines

Next, we estimated the abundance of potential translation template in transfected cells. For each of the six constructs (wt and 5 variants), 3 μg of RNA was transfected into HeLa cells, and at 0, 3, 6, 12, and 24 hours after transfection, RNA was harvested, immobilized on a slot-blot apparatus, and incubated with radio-labeled strand-specific CVB3 RNA probes. Representative autoradiographs for pH3 and IH2 RNAs are shown in Figure 3B. Band intensities were measured using ImageJ software, allowing quantitation of the changes in genomic and antigenomic RNA contents over time. At t=0, the band intensities of the genomic RNAs were comparable in the pH3 and IH2 samples, confirming that equal amounts of input RNA were applied. The positive-sense RNA signal in pH3 RNA-transfected cells dropped marginally in the first 3 hours, then increased at first gradually (6 and 12 hours), then dramatically (24 hours). In contrast, the positive-sense RNA signal in cells transfected with IH2 RNA decreased constantly. These data suggest that the pH3 RNA was successfully replicated within the transfected cells, while the IH2 RNA was not. This hypothesis is consistent with the appearance of anti-genomic (negative sense) RNA in cells transfected with pH3 RNA, but not in cells transfected with IH2 RNA (Figure 3B, right-hand panels). We conclude that the deletion of as few as 32 nt of the 5′ terminus of CVB3 prevents genome amplification. The results for the remaining four deletion mutants (not shown) were indistinguishable from IH2. Therefore, all five deletions limit the abundance of positive-sense RNA (potential translational template) in transfected cells; this provides one explanation for the absence of detectable virus proteins in cells transfected with RNAs IH2-IH6 (Figure 3A).

In vitro translation data suggest that the CVB3 IRES is larger than previously proposed, and is similar in size to its poliovirus counterpart

The absence of RNA amplification provided a convincing explanation for vaccine failure, but we wished to determine whether or not the deletions also had an effect on the ability of the individual RNA molecules to act as templates for translation. The five variant RNAs, and pH3 RNA as a positive control, were transcribed in vitro using T7 RNA polymerase, and were added to an *in vitro* translation reaction, as described in Materials and Methods. After a 4-hour incubation, the labeled proteins were analyzed by gel electrophoresis and autoradiography, and the resulting data are shown in Figure 4. As expected, abundant viral protein was produced from the pH3 RNA template. In addition, the IH2 and IH3 RNAs were translated at high efficiency; all major coxsackievirus bands including P1, P3, 3CD, 3D, 2BC, VP0, 2C, VP1, VP3, 3C, 2A, and 3AB are present in all three lanes representing pH3, IH2, and IH3. From this analysis, we cannot exclude minor effects of the IH2 and IH3 deletions because, when compared with the pH3 sample, the intensities of the VP0 and VP3 bands appear to slightly decline across these three samples. At present, we cannot explain this observation; one obvious possibility is a change in post-translational processing similar to a previous report from our laboratory (Harkins *et al.*, 2005), but the absence of the precursor protein, VP0-VP3, argues against this. Nevertheless, these data show that the first 75 residues of the CVB3 5′UTR can be removed without dramatically interfering with *in vitro* translation; this conflicts with previous *in vitro* translation data, which indicated that deletion of the first 63 nucleotides had

a profound negative effect (Yang *et al.*, 1997). In contrast to these possible minor effects, the deletion of a further 50 bases (IH4) causes a profound change in virus protein translation. This deletion completely abrogates protein synthesis from the RNA template, an outcome that is observed also in the remaining two deletion variants IH5 and IH6. Our approach, like the vast majority of published studies, does not directly measure ribosome entry/assembly, and instead relies on the end result, translation; but the resulting data strongly suggest that the 5′ boundary of the CVB3 IRES extends to between residues 76-125 of the viral 5′UTR, some 200-300 nt closer to the 5′ terminus than previously thought, and similar to the location identified in poliovirus.

Discussion

The 5′UTR of picornaviruses regulates not only translation, but also replication, and contributes to the control of viral pathogenesis and tissue tropism (Semler, 2004). A previous report indicated that a CVB3 RNA bearing a deletion of nt 1-249 in the 5′UTR, when transfected into HeLa cells, caused very little cytopathic effect (CPE) but still produced abundant viral protein (~50% of the wt level, Liu *et al.*, 1999), which appeared to be attributes of an ideal candidate RNA vaccine. For this reason, we prepared a number of similar deletion variant RNAs, lacking 32 to 209 nt from the CVB3 5′UTR (Figure 1). None of the RNA constructs gave rise to infectious virus, as expected (Figure 2A-C), and consistent with the earlier report. Surprisingly, however, nor did they confer any degree of protective immunity (Figure 2D). Our subsequent analyses provided a plausible explanation for their poor immunogenicity; none of the deletion RNA variants gave rise to a detectable level of viral protein within transfected cells (Figure 3A). This observation, in turn, could be attributed to two independent phenomena: all five RNAs were replication-defective, resulting in lower numbers of potential translation templates in transfected cells (Figure 3B); and the IH4-IH6 RNAs also showed defects in translation, consistent with the upstream boundary of the CVB3 IRES lying closer to the 5′ end than previously thought (Figure 4).

Analyses of the viral RNA content of transfected cells (Figure 3B) showed clearly that, in contrast to wt RNA, the quantity of positive-strand IH2-IH6 RNAs decreased over time, and antigenomic material was never detected. These findings provide a likely explanation for the failure of a 1-63 deletion mutant to cause a CPE in transfected cells (Liu *et al.*, 1999). We considered the possibility that the deleterious effects of the IH2-IH6 deletions resulted from destabilization and rapid degradation of these RNAs, rather than a direct inhibition of their replicative capacity. We cannot completely exclude RNA destabilization as a possible mechanism, but we believe it to be unlikely because the input IH2 RNA remained readily-detectable (albeit at decreasing amounts) over a period of 24 hours after transfection of tissue culture cells (Figure 3B), and the same degree of input RNA stability was observed for the IH3-6 RNAs (data not shown). Therefore, we conclude that the sequences at the immediate 5′ terminus of the CVB3 genome are required for RNA replication. To our knowledge, the importance these sequences to CVB replication has not been previously demonstrated. However, it can be argued that these findings are not surprising. The secondary RNA structure predicted in Figure 1B differs somewhat from a folding pattern previously proposed (Yang *et al.*, 1997; Liu *et al.*, 1999), mainly because the structure shown in Figure 1B contains a “cloverleaf” within the first ~100 nucleotides, rather than two separate stem-loops. At least four different approaches have indicated that this cloverleaf is likely to be present in the 5′UTR of CVB3. (i) A similar structure has been reported in several enterovirus and rhinovirus 5′ UTRs, and forms a ribonucleoprotein complex with the viral 3C polypeptide (Andino *et al.*, 1990; Leong *et al.*, 1993) or the 3CD precursor protein, as well as the host poly r(C) binding protein (PCBP) (Andino *et al.*, 1993). (ii) Circular dichroism data are consistent with a cloverleaf's being present in CVB3, and gel-shift assays (Zell *et al.*, 2002) together with NMR spectroscopy (Ohlenschlager *et al.*, 2004) indicate that the CVB3 3C protein binds to the fourth

stem-loop in the proposed structure. (iii) The formation of a nucleoprotein complex at the cloverleaf is an absolute requirement for polioviral RNA replication, suggesting that it may be important for CVB. (iv) A chimeric virus, in which poliovirus nucleotides 1-627 were replaced with the equivalent CVB sequence, showed biosynthetic properties similar to those of the parental poliovirus (Johnson and Semler, 1988), indicating that the poliovirus-encoded proteins interacted with a CVB-derived cloverleaf. These published data, although very strongly suggestive, do not definitively demonstrate a requirement for these 5′-terminal sequences in CVB replication; the data herein provide conclusive evidence that this is the case. Furthermore, our data take on additional significance in light of a recent, intriguing, report that CVB infection *in vivo* gives rise to 5′UTR deletion mutants that are very similar to those constructed herein; these naturally-occurring mutants cause no CPE and appear to replicate at low levels, and purified viral capsids contain a high proportion of negative-strand RNA (Kim *et al.*, 2005). We found no evidence that our deletion mutants gave rise to such viral variants, and our *in vivo* histological analyses (Figure 2C) suggested that the IH2-IH6 RNAs were non-pathogenic; but the approaches taken in our study may not have been sufficiently sensitive to have allowed the detection of these species.

Next, we evaluated the capacity of each of the six RNA templates to direct viral protein synthesis in a cell-free system, and found that IH2 & IH3 were relatively efficient, while IH4-IH6 were completely inactive (Figure 4). These data place the 5′ end of the CVB3 IRES somewhere between nt 76 and 125 from the genome 5′ terminus. The fact that our conclusions regarding the CVB3 5′UTR and IRES differ from those already published is, perhaps, less surprising than it might at first appear. An IRES often is presented as being a distinct block of contiguous sequence, with well-defined boundaries, but some sequence changes inside the IRES are well-tolerated, suggesting that the IRES itself is, to a greater or lesser extent, an assembly of discontinuous parts. Even for the prototypical IRES, in poliovirus, there remains some debate; this motif has been subjected to careful analyses by a number of laboratories and, although a consensus has emerged, fine details differ (Trono *et al.*, 1988;Pelletier *et al.*, 1988b;Nicholson *et al.*, 1991;Haller *et al.*, 1993). Contributing to the variability, many methods have been employed in mapping the functions of picornaviral 5′UTRs. Some are *in vivo*, others in tissue culture, and others still in cell-free systems. Some IRES mapping studies have used sequence insertions and deletions or linker scanning (Haller and Semler, 1992), others have used hybrid arrest of translation. Furthermore, IRES mapping often relies on somewhat indirect criteria to indicate ribosome binding/assembly. Some studies are based on the detection of viral proteins; others have employed the presence of absence of CPE as an indicator of IRES function (Liu *et al.*, 1999). In this study, we have used cell-free protein synthesis as the indicator of ribosome binding. Taken together, our data suggest strongly that the CVB3 IRES may be considerably larger than previously conceived, with its 5′ boundary lying at a location that is directly comparable with the equivalent poliovirus boundary. In summary, we conclude that a deletion of the first 32 or 75 nt of the CVB3 genome (IH2 and IH3) prevents RNA replication, but has little effect on the efficiency or fidelity of translation; and that deletion of an additional 50 nt (IH4) or more (IH5, 6) results in RNA molecules that are defective in both replication and translation. For these reasons, and because of the recent report that CVB bearing 5′ deletions may be able to persist *in vivo* (Kim *et al.*, 2005), such viral RNAs should not be considered as viable candidate vaccines.

Acknowledgements

We are grateful to Annette Lord for excellent secretarial support. This work was supported by NIH awards R01-AI-42314 (JLW) and F32-AI-065095 (CTC); and by American Heart Association award ID0225037Y (IPH). This is manuscript number 17661 from the Scripps Research Institute.

References

Andino R, Rieckhof GE, Achacoso PL, Baltimore D. Poliovirus RNA synthesis utilizes an RNP complex formed around the 5′-end of viral RNA. EMBO J 1993;12:3587–3598. [PubMed: 8253083]

Andino R, Rieckhof GE, Baltimore D. A functional ribonucleoprotein complex forms around the 5′ end of poliovirus RNA. Cell 1990;63:369–380. [PubMed: 2170027]

Arnesjo B, Eden T, Ihse I, Nordenfelt E, Ursing B. Enterovirus infections in acute pancreatitis. Scand J Gastroenterol 1976;11:645–649. [PubMed: 996429]

Cornell CT, Brunner JE, Semler BL. Differential rescue of poliovirus RNA replication functions by genetically modified RNA polymerase precursors. J Virol 2004;78:13007–13018. [PubMed: 15542652]

Daley AJ, Isaacs D, Dwyer DE, Gilbert GL. A cluster of cases of neonatal coxsackievirus B meningitis and myocarditis. J Paediatr Child Health 1998;34:196–198. [PubMed: 9588649]

Dan M, Chantler JK. A genetically engineered attenuated coxsackievirus B3 strain protects mice against lethal infection. J Virol 2005;79:9285–9295. [PubMed: 15994822]

Fohlman J, Pauksen K, Morein B, Bjare U, Ilback NG, Friman G. High yield production of an inactivated coxsackie B3 adjuvant vaccine with protective effect against experimental myocarditis. Scand J Infect Dis Suppl 1993;88:103–108. [PubMed: 8390713]

Gauntt CJ, Paque RE, Trousdale MD, Gudvangen RJ, Barr DT, Lipotich GJ, Nealon TJ, Duffey PS. Temperature-sensitive mutant of coxsackievirus B3 establishes resistance in neonatal mice that protects them during adolescence against coxsackievirus B3-induced myocarditis. Infect Immun 1983;39:851–864. [PubMed: 6299950]

Haller AA, Nguyen JH, Semler BL. Minimum internal ribosome entry site required for poliovirus infectivity. J Virol 1993;67:7461–7471. [PubMed: 8230467]

Haller AA, Semler BL. Linker scanning mutagenesis of the internal ribosome entry site of poliovirus RNA. J Virol 1992;66:5075–5086. [PubMed: 1321289]

Harkins S, Cornell CT, Whitton JL. Analysis of translational initiation in Coxsackievirus B3 suggests an alternative explanation for the high frequency of R_{+4} in the eukaryotic consensus motif. J Virol 2005;79:987–996. [PubMed: 15613327]

Henke A, Wagner E, Whitton JL, Zell R, Stelzner A. Protection of mice against lethal coxsackievirus B3 infection by using DNA immunization. J Virol 1998;72:8327–8331. [PubMed: 9733878]

Hunziker IP, Harkins S, Feuer R, Cornell CT, Whitton JL. Generation and analysis of an RNA vaccine that protects against coxsackievirus B3 challenge. Virol 2004;330:196–208.

Imrie CW, Ferguson JC, Sommerville RG. Coxsackie and mumpsvirus infection in a prospective study of acute pancreatitis. Gut 1977;18:53–56. [PubMed: 838403]

Jang SK, Krausslich HG, Nicklin MJ, Duke GM, Palmenberg AC, Wimmer E. A segment of the 5′ nontranslated region of encephalomyocarditis virus RNA directs internal entry of ribosomes during in vitro translation. J Virol 1988;62:2636–2643. [PubMed: 2839690]

Johnson VH, Semler BL. Defined recombinants of poliovirus and coxsackievirus: sequence-specific deletions and functional substitutions in the 5′-noncoding regions of viral RNAs. Virol 1988;162:47–57.

Kim KS, Tracy S, Tapprich W, Bailey J, Lee CK, Kim K, Barry WH, Chapman NM. 5′-Terminal Deletions Occur in Coxsackievirus B3 during Replication in Murine Hearts and Cardiac Myocyte Cultures and Correlate with Encapsidation of Negative-Strand Viral RNA. J Virol 2005;79:7024–7041. [PubMed: 15890942]

Kishimoto C, Hiraoka Y. Clinical and experimental studies in myocarditis. Curr Opin Cardiol 1994;9:349–356. [PubMed: 8049593]

Knowlton KU, Jeon ES, Berkley N, Wessely R, Huber SA. A mutation in the puff region of VP2 attenuates the myocarditic phenotype of an infectious cDNA of the Woodruff variant of coxsackievirus B3. J Virol 1996;70:7811–7818. [PubMed: 8892902]

Leong LE, Walker PA, Porter AG. Human rhinovirus-14 protease 3C (3Cpro) binds specifically to the 5′-noncoding region of the viral RNA. Evidence that 3Cpro has different domains for the RNA binding and proteolytic activities. J Biol Chem 1993;268:25735–25739. [PubMed: 8245010]

Liu Z, Carthy CM, Cheung P, Bohunek L, Wilson JE, McManus BM, Yang D. Structural and functional analysis of the 5′ untranslated region of coxsackievirus B3 RNA: In vivo translational and infectivity studies of full-length mutants. Virol 1999;265:206–217.

Meerovitch K, Nicholson R, Sonenberg N. In vitro mutational analysis of cis-acting RNA translational elements within the poliovirus type 2 5′ untranslated region. J Virol 1991;65:5895–5901. [PubMed: 1656078]

Mena I, Fischer C, Gebhard JR, Perry CM, Harkins S, Whitton JL. Coxsackievirus infection of the pancreas: evaluation of receptor expression, pathogenesis, and immunopathology. Virol 2000;271:276–288.

Modlin JF, Rotbart HA. Group B coxsackie disease in children. Curr Top Microbiol Immunol 1997;223:53–80. [PubMed: 9294925]

Nicholson R, Pelletier J, Le SY, Sonenberg N. Structural and functional analysis of the ribosome landing pad of poliovirus type 2: in vivo translation studies. J Virol 1991;65:5886–5894. [PubMed: 1656077]

Ohlenschlager O, Wohnert J, Bucci E, Seitz S, Hafner S, Ramachandran R, Zell R, Gorlach M. The structure of the stemloop D subdomain of coxsackievirus B3 cloverleaf RNA and its interaction with the proteinase 3C. Structure (Camb) 2004;12:237–248. [PubMed: 14962384]

Pelletier J, Kaplan G, Racaniello VR, Sonenberg N. Cap-independent translation of poliovirus mRNA is conferred by sequence elements within the 5′ noncoding region. Mol Cell Biol 1988a;8:1103–1112. [PubMed: 2835660]

Pelletier J, Kaplan G, Racaniello VR, Sonenberg N. Translational efficiency of poliovirus mRNA: mapping inhibitory cis- acting elements within the 5′ noncoding region. J Virol 1988b;62:2219–2227. [PubMed: 2836606]

Pelletier J, Sonenberg N. Internal initiation of translation of eukaryotic mRNA directed by a sequence derived from poliovirus RNA. Nature 1988;334:320–325. [PubMed: 2839775]

Ramsingh AI. Coxsackieviruses and Pancreatitis. Front Biosci 1997;2:e53–e62. [PubMed: 9257948]

Reyes MP, Lerner AM. Coxsackievirus myocarditis--with special reference to acute and chronic effects. Prog Cardiovasc Dis 1985;27:373–394. [PubMed: 2988014]

See DM, Tilles JG. Efficacy of a polyvalent inactivated-virus vaccine in protecting mice from infection with clinical strains of group B coxsackieviruses. Scand J Infect Dis 1994;26:739–747. [PubMed: 7747099]

Semler BL. Poliovirus proves IRES-istible in vivo. J Clin Invest 2004;113:1678–1681. [PubMed: 15199401]

Trono D, Andino R, Baltimore D. An RNA sequence of hundreds of nucleotides at the 5′ end of poliovirus RNA is involved in allowing viral protein synthesis. J Virol 1988;62:2291–2299. [PubMed: 2836612]

van Houten N, Bouchard PE, Moraska A, Huber SA. Selection of an attenuated Coxsackievirus B3 variant, using a monoclonal antibody reactive to myocyte antigen. J Virol 1991;65:1286–1290. [PubMed: 1847455]

Woodruff JF. Viral myocarditis. A review. Am J Pathol 1980;101:425–484. [PubMed: 6254364]

Yang D, Wilson JE, Anderson DR, Bohunek L, Cordeiro C, Kandolf R, McManus BM. In vitro mutational and inhibitory analysis of the cis-acting translational elements within the 5′ untranslated region of coxsackievirus B3: potential targets for antiviral action of antisense oligomers. Virol 1997;228:63–73.

Zell R, Sidigi K, Bucci E, Stelzner A, Gorlach M. Determinants of the recognition of enteroviral cloverleaf RNA by coxsackievirus B3 proteinase 3C. RNA 2002;8:188–201. [PubMed: 11911365]

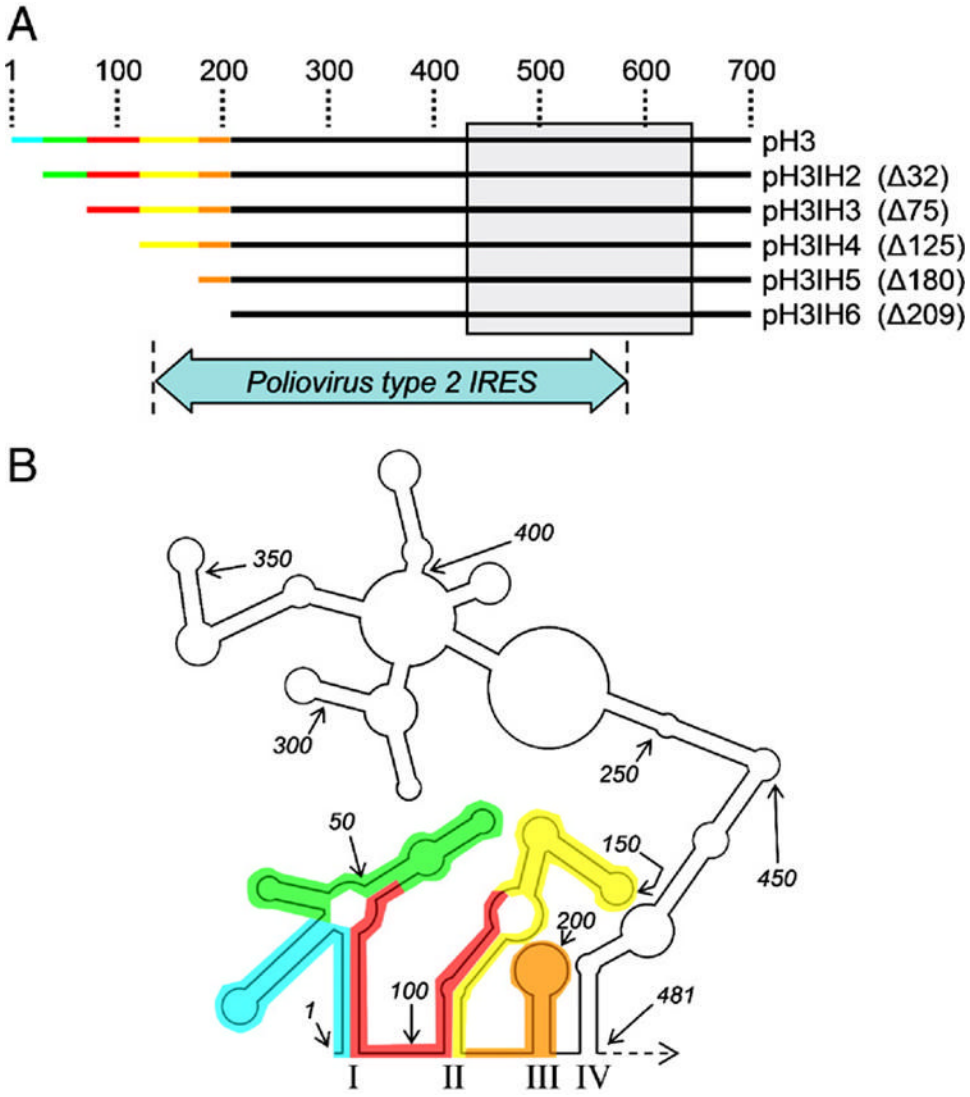

Figure 1. The five deletions used to evaluate functional elements in the CVB3 5′UTR, and their impact on predicted RNA folding motifs

Panel A. The sequences involved in each of the 5 deletions in the CVB3 5′UTR are shown in color, and the numbers of bases missing (Δ) in each of the IH2-IH6 series are shown in parentheses. The grey box indicates the core of the CVB3 IRES, as indicated by published studies (Liu *et al.*, 1999), and the arrow demonstrates the approximate location of the poliovirus type 2 IRES (Nicholson *et al.*, 1991). *Panel B* presents a cartoon of the predicted folding of the first 481 nt of the CVB3 genome, according to the Zuker algorithm (see text). The numerals indicate the number of nt from the 5′ terminus of the genome, the regions affected by each deletion are color-coded to correspond with panel A, and IRES stem-loops I-IV are indicated.

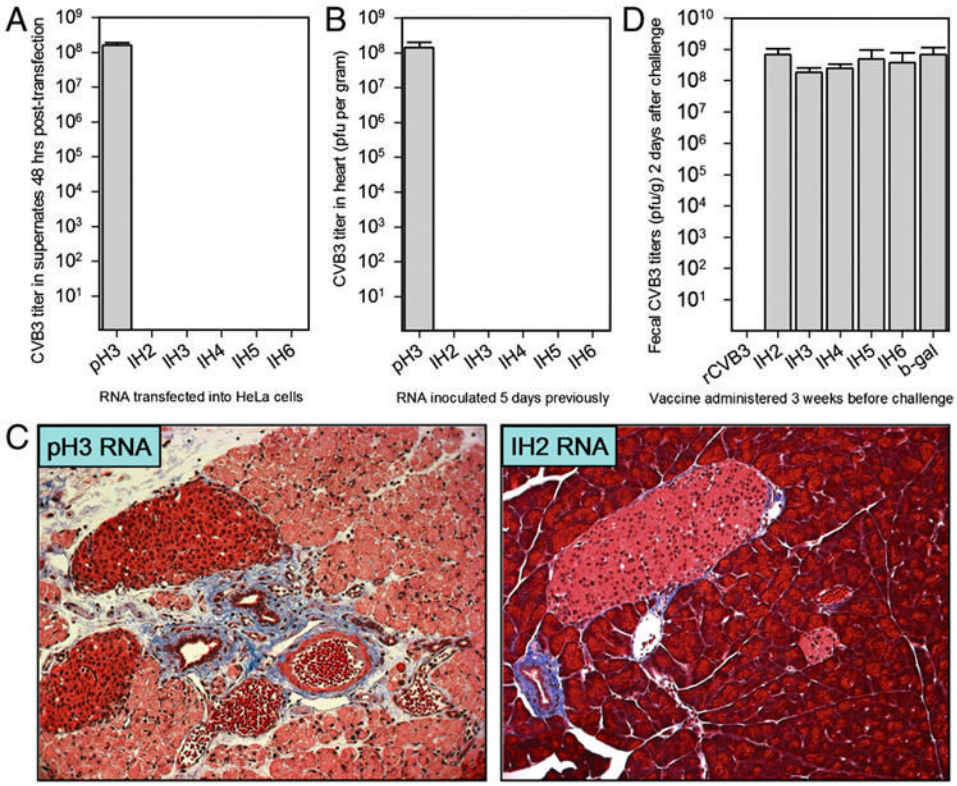

Figure 2. Deletions in the 5′UTR prevent production of infectious virus, but also abrogate protective efficacy

Panel A. HeLa cells were transfected with 3 μg of the indicated RNAs and, 48 hours later, supernatants were harvested. The titers (if any) of infectious virus are shown. *Panel B.* C57BL/6 mice (4/group) were injected with 15 μg of the indicated RNAs and, 5 days later, the mice were sacrificed, and virus titers were determined in hearts, spleens, and pancreata. The heart titers are shown (pfu/gram) and are representative of the titers in the other organs. *Panel C.* Representative histological samples of the pancreata from mice infected with pH3 RNA (left) or IH2 RNA (right) are shown (stained with Masson's trichrome). Marked inflammatory infiltrates and acinar cell destruction are evident in the former sample, while the latter tissue appears histologically normal. *Panel D.* Mice (4/group) were immunized, and boosted once, with the indicated vaccines (see text for details) and, 3 weeks after the boost, were challenged with 8000 pfu of wild type CVB3 (H3). Two days post-infection, feces were collected, and the virus titers therein are shown (pfu/gram).

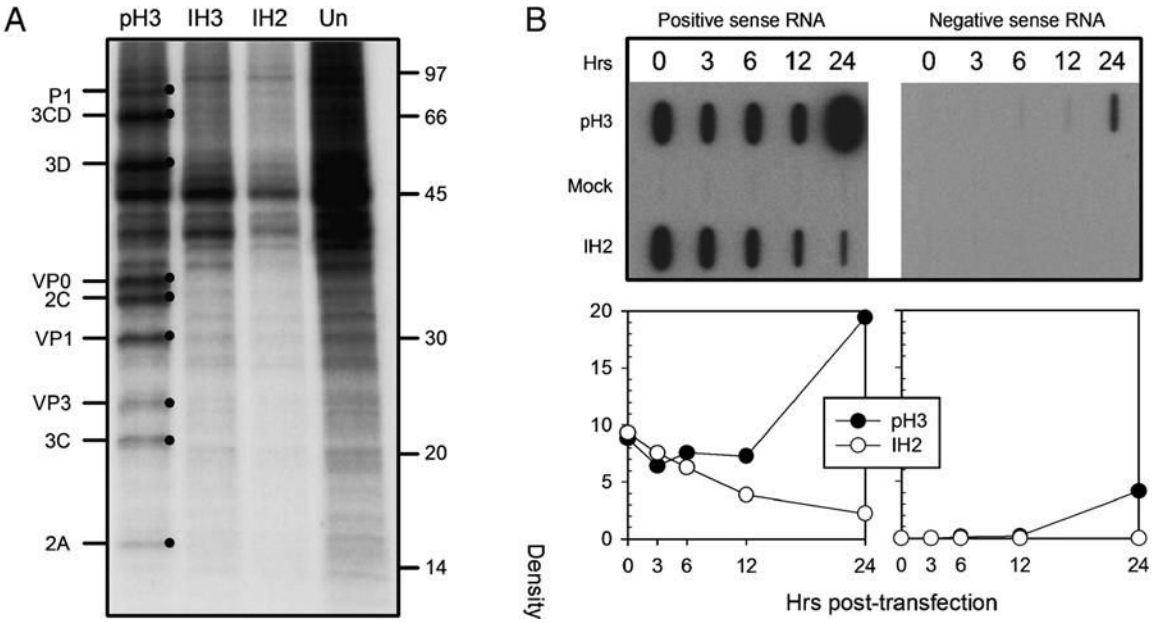

Figure 3. The effects of deletions in the 5′UTR on viral protein synthesis, and on RNA replication, in transfected cells

Panel A. HeLa cells were transfected with each of the indicated RNAs, or were left unmanipulated (Un). Newly-synthesized proteins were radiolabeled using S35 methionine (see Materials and Methods) and, following cell disruption, were separated on a polyacrylamide gel, which was subjected to autoradiography. Virus protein sizes are indicated to the left, and are highlighted by dots in the pH3-transfected extract. *Panel B.* HeLa cells were transfected with pH3 or IH2 RNAs, or were mock-transfected, and RNA was extracted at the indicated 5 time points. The amounts of positive-sense (left panel) and negative-sense (right panel) RNAs present at each time point was determined by slot blot. The density of each signal was measured using ImageJ, and the results (arbitrary units) are shown in the lower graphs.

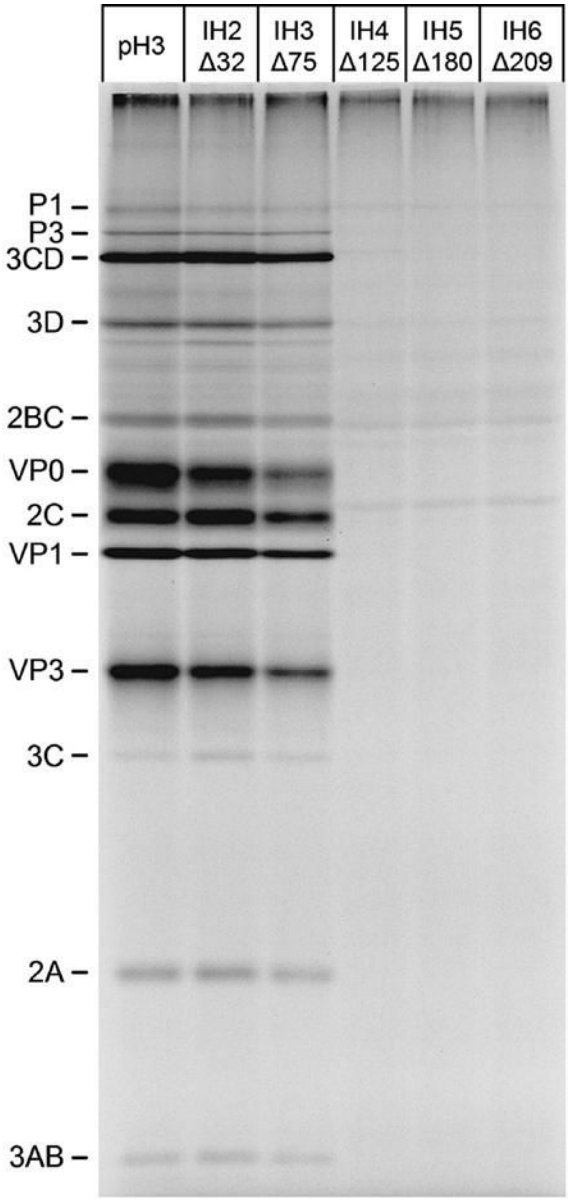

Figure 4. In vitro translation indicates that the CVB3 IRES is larger than previously determined, and is similar in extent to that of poliovirus

Each of the six indicated uncapped RNAs was incubated for 4 hours in an *in vitro* translation reaction, carried out in the presence of ^{35}S-methionine, and aliquots of reaction mixtures were analyzed by polyacrylamide gel electrophoresis followed by autoradiography. The extent of each of the 5 deletions is shown above each lane (Δ), and the position of each virus protein is shown on the left side.